MOLECULAR AND CELLULAR BIOLOGY, Aug. 2006, p. 5715–5727 Vol. 26, No. 15
0270-7306/06/$08.00+0 doi:10.1128/MCB.00001-06

MafB Is Essential for Renal Development and F4/80 Expression in Macrophages

Takashi Moriguchi,[1,6]† Michito Hamada,[1]† Naoki Morito,[1] Tsumoru Terunuma,[1] Kazuteru Hasegawa,[1] Chuan Zhang,[1] Tomomasa Yokomizo,[1] Ritsuko Esaki,[1] Etsushi Kuroda,[5] Keigyou Yoh,[3] Takashi Kudo,[1] Michio Nagata,[1] David R. Greaves,[7] James Douglas Engel,[6]* Masayuki Yamamoto,[1,4] and Satoru Takahashi[1,2]

Institute of Basic Medical Sciences,[1] Laboratory Animal Resource Center,[2] Institute of Clinical Medicine,[3] and Center for Tsukuba Advanced Research Alliance,[4] University of Tsukuba, Tsukuba 305-8575, Japan; Department of Immunology, University of Occupational and Environmental Health, School of Medicine, Kitakyushu 807-8555, Japan[5]; Department of Cell and Developmental Biology, University of Michigan, Ann Arbor, Michigan 48109-0616[6]; and Sir William Dunn School of Pathology, University of Oxford, Oxford OX1 3RE, United Kingdom[7]

Received 1 January 2006/Returned for modification 22 February 2006/Accepted 8 May 2006

MafB is a member of the large Maf family of transcription factors that share similar basic region/leucine zipper DNA binding motifs and N-terminal activation domains. Although it is well known that MafB is specifically expressed in glomerular epithelial cells (podocytes) and macrophages, characterization of the null mutant phenotype in these tissues has not been previously reported. To investigate suspected MafB functions in the kidney and in macrophages, we generated *mafB*/green fluorescent protein (GFP) knock-in null mutant mice. *mafB* homozygous mutants displayed renal dysgenesis with abnormal podocyte differentiation as well as tubular apoptosis. Interestingly, these kidney phenotypes were associated with diminished expression of several kidney disease-related genes. In hematopoietic cells, GFP fluorescence was observed in both Mac-1- and F4/80-expressing macrophages in the fetal liver. Interestingly, F4/80 expression in macrophages was suppressed in the homozygous mutant, although development of the Mac-1-positive macrophage population was unaffected. In primary cultures of fetal liver hematopoietic cells, MafB deficiency was found to dramatically suppress F4/80 expression in nonadherent macrophages, whereas the Mac-1-positive macrophage population developed normally. These results demonstrate that MafB is essential for podocyte differentiation, renal tubule survival, and F4/80 maturation in a distinct subpopulation of nonadherent mature macrophages.

The product of the c-*maf* proto-oncogene and its relatives (the large Maf family of transcription factors) share conserved basic regions and amphipathic helices (bZip) that mediate DNA binding to Maf recognition elements (MAREs) (20, 21) and dimer formation, respectively. The large Maf proteins MafA/L-Maf/SMaf, MafB, c-Maf, and NRL each contain an acidic domain that promotes transcriptional activation, and each protein has been shown to play key roles in cellular differentiation (19–22, 33, 36, 44, 46, 50).

MafB deficiencies were originally reported to be responsible for the phenotypes observed in the *Kreisler* mutant mouse. The *Kreisler* mutation was an X-ray-induced chromosomal inversion that led to abrogated MafB expression, specifically in the fifth and sixth rhombomeres of the embryonic hindbrain (8). Hindbrain-specific *mafB* loss of function in the *Kreisler* mutant led to aberrant segmentation and subsequent hyperactive behavior (characterized by head tossing and running in circles as a consequence of an inner ear defect). In all other tissues and organs (in embryos at 8.5 days postcoitum through adulthood), MafB expression was conserved and equivalent in wild-type and *Kreisler* mutant animals (13). Analysis of mice homozygous for a second mutant allele of *mafB* (called kr^{ENU}) showed that it is also expressed in glomerular visceral epithelial cells (podocytes) and is required for renal foot process formation (39). The kr^{ENU} mutation, an Asn-to-Ser substitution at residue 248 within the MafB DNA binding domain, reduced MafB binding activity without affecting the stability of the MafB protein (39). The less severe hindbrain phenotype observed in kr^{ENU} mice suggested that it was a mild hypomorphic allele of the original *mafB* gene (39).

MafB is expressed selectively in monocytes and macrophages but not in other hematopoietic lineages distinct from many other myeloid transcription factors (13, 44). During macrophage differentiation, MafB is not expressed in multipotent progenitors, but it is expressed at moderate levels in myeloblasts and is strongly induced in mature monocytes and macrophages (44). It has previously been reported that MafB is both necessary and sufficient to induce myelomonocytic differentiation of transformed avian myeloblast cells in vitro (23). MafB is known to interact with Ets-1, a helix-turn-helix transcription factor, and to inhibit Ets-1 *trans*-activation activity, thereby interfering with erythroid differentiation (44). These results strongly suggested that MafB could be a key regulator of lineage determination during myelopoiesis, but in vivo verification of this hypothesis has not been forthcoming.

Since both the *Kreisler* and kr^{ENU} mutants retain residual MafB function, the consequences of complete MafB inactivation are unknown. Recently, Blanchi et al. reported that *mafB*

* Corresponding author. Mailing address: Department of Cell and Developmental Biology, University of Michigan, Ann Arbor, Michigan 48109-0616. Phone: (734) 615-7248. Fax: (734) 615-7856. E-mail: engel@umich.edu.

† T.M. and M.H. contributed equally to this work.

null mutant mice displayed defective respiratory rhythmogenesis (4), while the biological consequences of the null mutation in other tissues and organs were not addressed. Furthermore, the expression of MafB within the panoply of hematopoietic cells has not yet been fully documented. To address these issues, we generated *mafB* mutant mice in which the green fluorescent protein (GFP) gene was inserted into the *mafB* locus by homologous recombination. GFP expression recapitulates the expression of endogenous MafB, thus facilitating the analysis of MafB-expressing cell lineages and the identification of functional abnormalities that might result as a consequence of MafB loss of function. We report here that *mafB* homozygous mutant mice display severe renal dysgenesis, characterized by abnormal glomerular differentiation and nephric tubular apoptosis associated with the diminished expression of several kidney disease-related genes. In addition, MafB expression was observed in specific subpopulations of differentiated macrophages in vivo, and its deficiency significantly suppressed F4/80 transcription in nonadherent mature macrophages.

MATERIALS AND METHODS

Construction of the *mafB* targeting vector. To disrupt the *mafB* gene and simultaneously examine the tissue distribution of MafB expression, mice in which the GFP gene was inserted into the chromosomal *mafB* locus were generated. The targeting vector was constructed using genomic DNA from a 129SV/J mouse library (Stratagene, La Jolla, CA) recovered by screening with a mouse MafB cDNA probe. We subcloned an 8.2-kbp genomic SacI fragment spanning from −7.8 kbp to +364 bp relative to the transcription initiation site of the gene that was then ligated into the GFP gene in pCMX-SAH/Y145F (30). The 3′ end of the GFP expression cassette was joined to a *neo* gene cassette flanked by *loxP* sequences, followed by a 2.5-kbp XhoI/EcoRI fragment of 129SV/J *mafB* DNA (Fig. 1A). This construct was then joined to a thymidine kinase expression cassette at the 3′ end and inserted between the XhoI and NotI sites of pBluescript (Stratagene, La Jolla, CA).

Generation of *mafB* null mutant mice. The targeting vector was linearized by NotI digestion and electroporated into E14 embryonic stem cells (17). Colonies resistant to double selection with G418 and ganciclovir were picked, expanded, and analyzed by PCR. A pair of primers (sense, 5′-AGTCACCCAAGGCCCTCCAGCCTCTAATCT-3′; antisense, 5′-AGCAGCCGATTGTCTGTTGTGCCCAGTCAT-3′) that amplify a 3.0-kbp fragment composed of part of the 129SV/J *mafB* 3′-flanking region and the *neo* gene cassette was used for screening. PCR-positive clones were subsequently verified by Southern blotting. Homologous recombinant clones were injected into blastocysts of C57BL/6J mice. Male mice chimeric for the targeted allele were mated with C57BL/6J wild-type females, and heterozygous F1 (+/−Neo) mice were then crossed to Ayu1-Cre mice, a general deleter Cre recombinase-expressing transgenic line (34), to remove the Neo cassette. The resultant heterozygotes bearing the targeted allele were subsequently interbred to yield wild-type (+/+), heterozygous (+/−), and homozygous (−/−) *mafB* null mutant mice. Genotypes were determined by genomic Southern blotting (Fig. 1B and C) and PCR analysis of tail DNA. For amplification of the wild-type allele, sense and antisense primer pairs within the coding region of the mouse *mafB* gene were used; a primer pair specific for enhanced GFP cDNA was used to detect the mutant allele (Table 1). All experiments were performed according to the guide for the care and use of laboratory animals of the University of Tsukuba.

Histological analysis. Tissues and embryos were fixed in 4% paraformaldehyde in phosphate-buffered saline overnight and then processed for paraffin or frozen sections. Paraffin sections (8 to 12 μm) were cut with a microtome and processed for either hematoxylin and eosin or periodic acid-Schiff staining. For immunohistochemical analysis of GFP, MafB, and F4/80 expression, paraffin or frozen sections were incubated with a 1:1,000 dilution of rabbit polyclonal anti-GFP antibody (A-6455; Molecular Probes, Eugene, OR), anti-MafB (BL658; BETHYL Laboratories, Inc.), or rat polyclonal anti-mouse F4/80 (MCA497R; Serotec, Ltd., Oxford, United Kingdom). Immunoreactivity was visualized with avidin-biotin-peroxidase (Vector Laboratories, Burlingame, CA) in 0.01 M imidazole acetate buffer containing 0.05% 3,3′-diaminobenzidine tetrahydrochloride, 0.005% H_2O_2, and 2.5% $NiNH_4SO_4$. In costaining for MafB and F4/80, immunoreactivity was distinguished by brown (without $NiNH_4SO_4$) and black (with $NiNH_4SO_4$) reaction products, respectively. In situ hybridization for MafB and immunohistochemistry with antinephrin and antipodocin antibodies (Chemicon International, Inc., Temecula, CA) were performed as previously described (16, 22, 42). The MafB in situ probe was transcribed from pBluescript containing the full-length coding sequence. Terminal deoxynucleotidyltransferase-mediated dUTP-biotin nick end-labeling (TUNEL) assays were performed on paraffin-embedded sections utilizing an in situ apoptosis detection kit (Takara, BIOTECH, Otsu, Japan). For quantitative histological analysis, we counted TUNEL-positive cells in periglomerular areas of 20 randomly selected glomeruli and 20 randomly selected fields of cortical interstitium using a light microscope (magnification, ×400), and results are expressed as the apoptotic cell number/20 fields. For each genotype, one middle section from each of four kidneys of two pups was analyzed. The data were recorded as means ± standard deviations (SD). The statistical significance of the differences was determined by Student's *t* test. For electron microscopy, tissues were fixed in 2% glutaraldehyde in phosphate-buffered saline, and transmission electron microscopy was performed using standard methods.

RT-PCR, Northern blotting, real-time quantitative PCR, and serum creatinine analysis. The kidneys of newborn littermates were dissected, and total RNA was extracted using ISOGEN (Nippon Gene, Tokyo, Japan). Reverse transcription-PCR (RT-PCR) analysis of MafB mRNA was performed as previously described by using the primer pair shown in Table 1 (15). Real-time PCR analysis of F4/80 was performed using an ABI PRISM7700 apparatus (Perkin-Elmer), and F4/80 mRNA levels were quantitatively measured and normalized to glyceraldehyde-3-phosphate dehydrogenase (GAPDH) levels as previously described (45) (Table 1). For Northern blotting, 10 μg of total kidney RNA was electrophoresed on a denaturing formaldehyde gel and then blotted (in 20× SSC [1× SSC is 0.15 M NaCl plus 0.015 M sodium citrate]) onto a nylon membrane (Zeta-Probe GT; Bio-Rad) overnight. Those membranes were hybridized with the probes generated by RT-PCR using the primer pairs described in Table 1. Band intensities were quantified using ImageQuant version 5.2 software (Molecular Dynamics) and then normalized to GAPDH expression levels. Three independent animals of each genotype were analyzed. The concentrations of serum creatinine were measured by an automated analyzer for routine laboratory tests (DRY-CHEM 3500; Fuji Film, Inc., Tokyo, Japan). For statistical analysis, pairwise comparisons were made by Student's *t* test or Mann-Whitney U test using Stat View for Macintosh version 5.0 software (SAS Institute, Cary, NC).

Flow cytometric analysis of fetal/newborn hematopoietic cells. Fetal/newborn livers, spleens, and peripheral blood cells were isolated from each genotype of newborn littermates. Most erythrocytes were removed by specific gravity centrifugation with HISTOPAQUE-1083 (Sigma, St. Louis, MO). The remaining white blood cells were washed once in ice-cold phosphate-buffered saline. Nonspecific binding was blocked by incubation in 5% mouse serum for 15 min, followed by incubation with antibody for 10 min. Phycoerythrin (PE) or antigen-presenting cell (APC)-conjugated anti-Mac-1, anti-Gr-1, anti-CD4, anti-CD8, anti-CD19, anti-Ter119 (Pharmingen, San Diego, CA), anti-F4/80 (MCA497PE; Serotec, Ltd, Oxford, United Kingdom), and anti-major histocompatibility complex (MHC) class II (12-5321; eBioscience) antibodies were used. Flow cytometric analysis was performed with FACSCalibur and Vantage (Becton Dickinson, Mountain View, CA), and the data were analyzed using CellQuest software.

Generation of macrophages from fetal liver cells. Macrophages were derived from day 14.5 fetal livers of $mafB^{-/-}$, $mafB^{+/-}$, and $mafB^{+/+}$ mice. Suspensions of single fetal liver cells were prepared by mechanical disruption (grinding with a syringe insert against a 70-μm nylon cell strainer; BD Biosciences, Franklin Lakes, NJ). A total of 10^6 cells in suspension were centrifuged at 1,200 rpm for 5 min, and the cell pellet was resuspended in Dulbecco's modified Eagle's medium (high glucose, endotoxin tested; Life Technologies, Rockville, MD) supplemented with 10% fetal calf serum (heat inactivated), streptomycin and penicillin (100 units/ml), and macrophage colony-stimulating factor (M-CSF) (10 ng/ml) and then seeded either onto an adhesive tissue culture dish (catalog no. 353003; Falcon) or onto nonadhesive dishes coated with hydrophilic polymers (Hydrocell; Cell Seed, Tokyo). The culture medium was not changed throughout the experiment. M-CSF (final concentration, 10 ng/ml) was added every day from day 4 onwards. One, 2, 4, and 6 days after seeding, the cells were harvested and analyzed by flow cytometry. For the semisolid medium culture, 10^5 cells were pelleted and then resuspended in Methocult M3231 (StemCell Technologies Inc.) supplemented with M-CSF (100 ng/ml). Fourteen days after seeding, the cells were washed away from the methylcellulose and analyzed by fluorescence-activated cell sorter analysis.

Mammalian cell culture and transient transfection assays. The pGL3Basic-based 668-bp human F4/80 promoter luciferase construct was reported previously (37). A full-length MafB cDNA was subcloned into the pcDNA3.1+neo eukaryotic expression plasmid (Invitrogen). Murine macrophage cell line

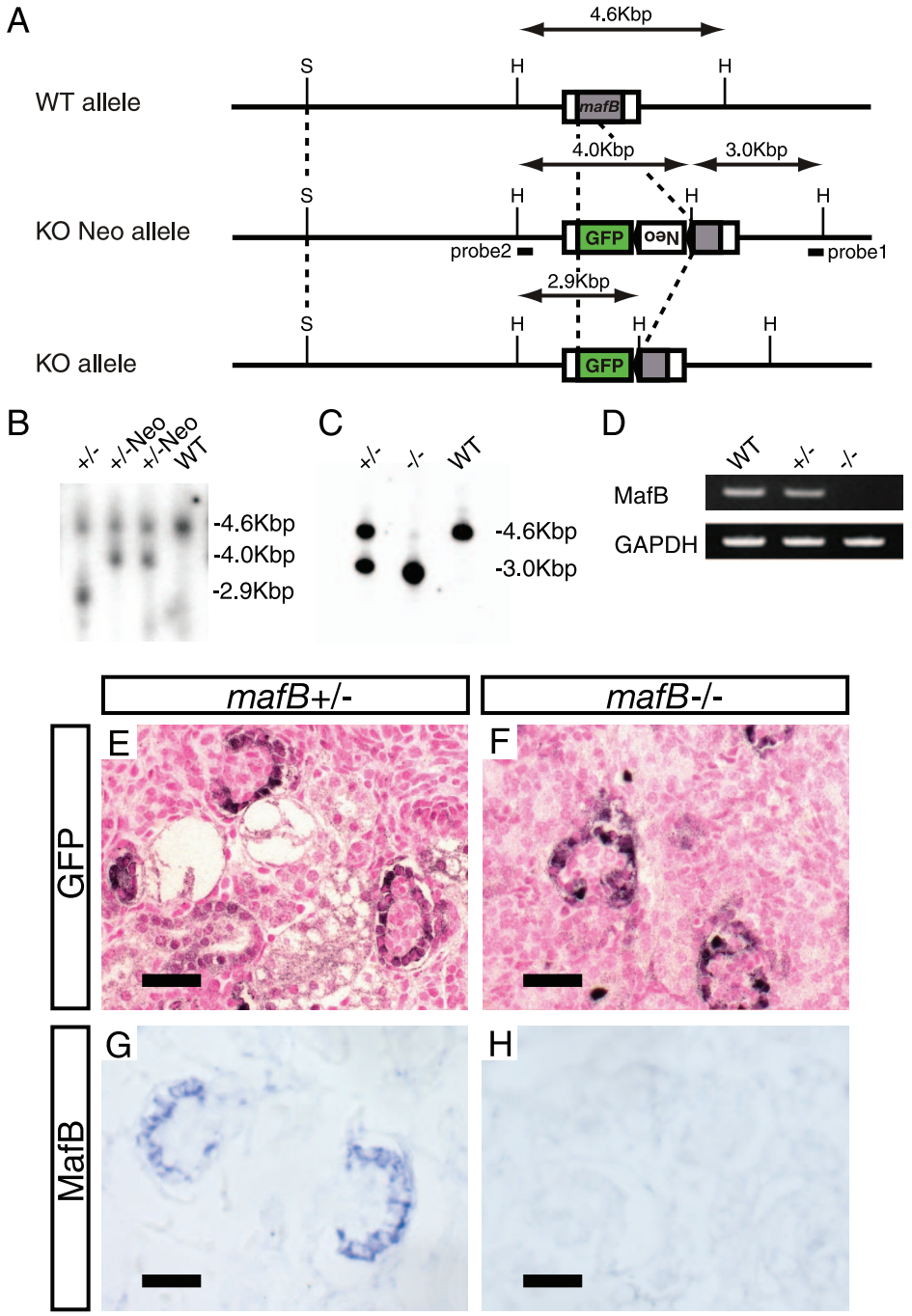

FIG. 1. Generation of *mafB* null mutant mice. (A) Strategy for GFP reporter gene knock-in to the *mafB* locus by homologous recombination. H and S are abbreviations for restriction enzyme cleavage sites for HindIII and SacI, respectively. Neo indicates the neomycin resistance gene flanked by *loxP* elements. The positions of the 3′ genomic probe 1 and internal probe 2 used for Southern blot analysis are indicated by the horizontal bar. (B) The HindIII restriction fragments detected with internal probe 2 in the wild type (WT) (4.6 kbp), knockout (KO) Neo allele (4.0 kbp), and KO allele (2.9 kbp) are indicated. (C) Genotyping by Southern blotting. HindIII digestion of genomic DNA extracted from the tails of sibling pups of each genotype generated 4.6-kbp and 3.0-kbp bands for the wild-type and KO alleles, respectively, using 3′ genomic probe 1. (D) RT-PCR analysis of MafB mRNA. RNA was prepared from the kidneys of wild-type and heterozygous and homozygous mutant *mafB* neonates. (E and F) GFP immunoreactivity in podocytes of $mafB^{+/-}$ and $mafB^{-/-}$ neonates. (G and H) Endogenous MafB mRNA expression was specifically detected in the podocytes of $mafB^{+/-}$ kidneys, whereas $mafB^{-/-}$ neonatal kidneys had no MafB mRNA accumulation. Scale bars represent 20 μm in all panels.

RAW264.7 was maintained in Dulbecco's modified Eagle's medium supplemented with 10% fetal bovine serum. Cells were transfected by lipofection using FuGENE6 transfection regent (Roche) and then harvested 24 h posttransfection. Luciferase assays were performed using the dual-luciferase reporter assay system (Promega). Transfection efficiencies were normalized to cotransfected, coexpressed *Renilla* luciferase activity.

RESULTS

Generation and molecular characterization of $mafB^{-/-}$ mice. In order to both disrupt the *mafB* gene in embryonic stem cells and enable the examination of its sites of expression in mice, a

TABLE 1. Sequences of primers used in genotyping and RT-PCR

Gene[a]	Primer	
	Sense	Antisense
MafB	TGAGCATGGGGCAAGAGCTG	CCATCCAGTACAGGTCCTCG
eGFP	AAACGGCCACAAGTTCAG	GAAGTTCACCTTGATGCC
Nephrin	GACCGGGACACAAGAAGCTC	GATGTCCCCTCAGCTCGAAG
Podocin	CATGTGTCCAAAGCCATCCA	CTTTTCCCCTTCTGCAGCAA
CD2AP	CGAGTTGGGGAAATCATCAG	TGAGGTAGGGCCAGTCAAAG
NEPH1	GGGGCTTCTTGATTGAAGAC	GTCACTGACTTCAGCAACAG
Pod1	TGCTGAGCAAGGCCTTCTCC	TGGCGGTCACCACTTCCTT
mFuc-TX	CAACAGCTGGGTCTTCAGTC	AGATCCCAGCTGATGTCTCT
Uromodulin	AGGACAGTTGTCCACGTACA	AGATGCTCAGGAGCCTCAAG
c-Myc	CTCCTCGAGCTGTTTGAAGGC	TGAAGGTCTCGTCGTCAGGATC
Podocalyxin	CCTCCAGGCCCCAGC	CCCAGCTTCATGTCACTGACT
F4/80	CCCAGCTTATGCCACCTGCA	TCCAGGCCCTGGAACATTGG
GAPDH	AAGGTCGGAGTCAACGGATT	TTGATGACAAGCTTCCCGTT

[a] eGFP, enhanced GFP.

targeting construct that would replace the coding sequence of *mafB* with GFP was generated (Fig. 1A). Homologous recombination was confirmed by genomic Southern blotting (data not shown). Three independent clones were injected into C57BL/6J blastocysts to generate chimeric offspring. Male chimeras were mated with C57BL/6J females to obtain heterozygous mutants, and the heterozygous animals were then crossed with Ayu-1 Cre mice that ubiquitously express Cre recombinase (34) to remove the neomycin resistance cassette (that was flanked by *loxP* sites). These heterozygotes (+/−) were interbred to generate homozygous $mafB^{-/-}$ mice. Neo gene excision and progeny genotypes were confirmed by Southern analysis of tail DNA (Fig. 1B and C).

To verify that the targeted mutagenesis resulted in the generation of a genuine null allele, we performed RT-PCR analyses of kidney mRNA recovered from neonates generated from heterozygous intercrosses. Unlike wild-type or heterozygous mutant kidneys that express high levels of MafB mRNA, $mafB^{-/-}$ neonatal kidneys lacked detectable MafB transcript (Fig. 1D). We observed the expected Mendelian ratios of wild-type, heterozygous, and homozygous mutant progeny at all stages of embryonic development and at birth (Fig. 1C and data not shown). However, all of the $mafB^{-/-}$ neonates died within 24 h after birth. A variety of morphological abnormalities, including cystic malformation of the inner ear (strikingly similar to the phenotype of the *Kreisler* mutant), was observed in $mafB^{-/-}$ neonates but not in their heterozygous siblings (data not shown) (38).

We next examined endogenous MafB expression in the newborn kidney. MafB transcripts were observed specifically in the podocytes of heterozygous neonates, whereas none were detected in homozygous mutants (18, 39) (Fig. 1G and H). GFP immunoreactivity was observed in the podocytes of heterozygous animals in the same pattern as MafB, and the same pattern was observed in the podocytes of homozygous *mafB* mutants (Fig. 1E and F). These observations demonstrate that the germ line gene targeting indeed created a *mafB* null allele, that GFP expression fully recapitulates endogenous MafB expression, and that podocytes are generated in *mafB* null mutant mice.

Renal dysgenesis in *mafB*-deficient mice. The renal vesicle, from which the nephron arises, proceeds through four morphologically well-defined stages: the comma-shaped body, the S-shaped body, the capillary loop, and the mature stages (1). Previous studies reported that MafB mRNA is expressed exclusively in the podocytes at the capillary loop stage and in the mature glomerulus, which are located more internally relative to the immature renal vesicles formed in the nephrogenic zone at the outer margin of the cortex (39).

Neonatal kidneys from homozygous *mafB* mutant mice displayed punctuate surface hemorrhages and a dystrophic appearance, unlike heterozygous mutant neonatal kidneys (Fig. 2A). Histological analysis revealed that the newborn homozygous mutant kidneys had relatively fewer differentiated mature glomeruli and displayed tubular dysgenesis accompanied by cyst formation, primarily in the area of proximal tubuli, in comparison to heterozygous mutants (Fig. 2C to F). In electron microscopic analysis of mature glomeruli, the podocytes of homozygous *mafB* mutant mice displayed a dearth of normal foot processes (Fig. 2H). The podocyte foot processes in the kidneys of the homozygous mutants were fused and did not interdigitate, whereas discrete foot processes were observed in the glomeruli of kidneys recovered from heterozygous littermates (Fig. 2G and H). Furthermore, we observed no urine collection in the bladder of homozygous mutant newborns, likely as a consequence of this tubular dysgenesis (data not shown).

To further evaluate renal function in *mafB* homozygous mutants, we carried out serum creatinine analysis. The mean serum creatinine concentration in homozygous mutant neonates (0.567 ± 0.082 mg/dl) was significantly higher than that in their heterozygous littermates (0.400 ± 0.063 mg/dl; $P = 0.0082$, Mann-Whitney U test) (Fig. 2B). Thus, *mafB* homozygous mutant newborns displayed clear evidence of renal dysfunction. These observations demonstrate that MafB is required for normal glomerular and tubular development and function.

Repression of kidney disease genes in *mafB* homozygous mutant mice. Recent advances in the study of human kidney disease have identified several key molecules that are required for podocyte development and glomerular function. The slit diaphragm, which laterally joins podocyte foot processes, is a

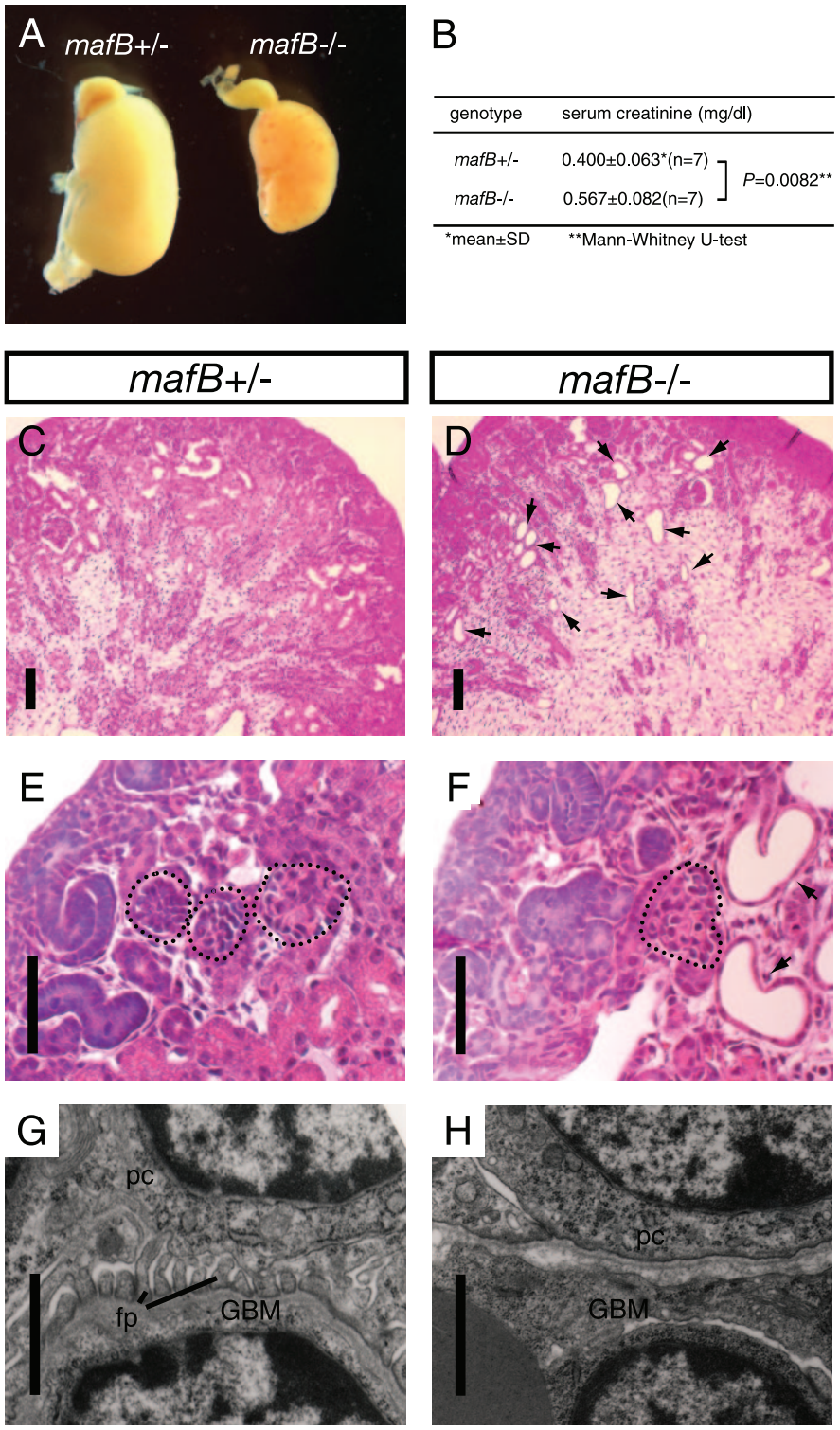

FIG. 2. Kidney abnormalities in *mafB*$^{-/-}$ neonatal mice. (A) Gross appearance of a neonatal kidney from a *mafB*$^{-/-}$ mouse. The *mafB*$^{-/-}$ kidney (right) has a punctate surface hemorrhage and a dystrophic general appearance, unlike kidneys recovered from a *mafB*$^{+/-}$ littermate (left). (B) *mafB*$^{-/-}$ mice display a significant difference from *mafB*$^{+/-}$ littermates in mean serum creatinine concentration ($P = 0.0082$, Mann-Whitney U test). (C and D) periodic acid-Schiff staining of *mafB*$^{+/-}$ and *mafB*$^{-/-}$ neonatal kidneys. (C) Tissue sections of *mafB*$^{+/-}$ kidneys showed numerous proximal and distal tubules. (D) Kidneys from *mafB*$^{-/-}$ mice have a reduced number of proximal and distal tubules accompanied by numerous cysts, primarily in the area of proximal tubuli (arrows in panels D and F). (E and F) *mafB*$^{+/-}$ kidneys had mature glomeruli, whereas kidneys from *mafB*$^{-/-}$ animals had fewer mature glomeruli (outlined by dotted lines). (G and H) Lack of normal podocyte foot processes in *mafB*$^{-/-}$ glomeruli. Electron microscopy revealed that *mafB*$^{-/-}$ podocyte foot processes were fused and did not interdigitate (H), whereas normal discrete foot processes were observed in the glomeruli of *mafB*$^{+/-}$ kidneys (G). pc, podocyte; fp, foot process; GBM, glomerular basement membrane. The scale bars in panels C, D, E, and F are 60 μm, whereas those in panels G and H represent 1 μm.

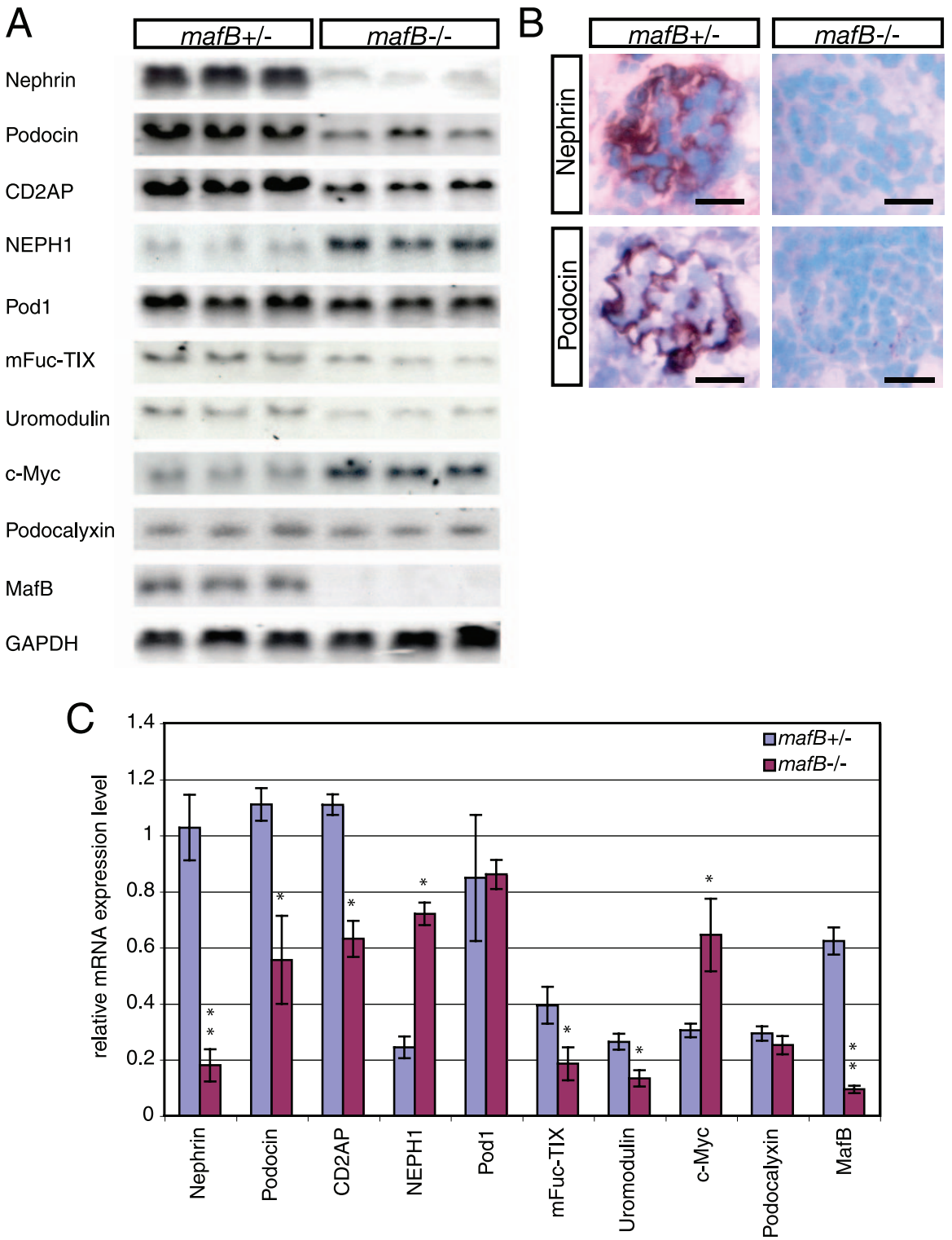

FIG. 3. Expression of kidney disease-related genes in *mafB* mutant mice. (A) *mafB* homozygous mutant kidneys displayed a significant reduction in the accumulation of kidney disease-related mRNAs (nephrin, podocin, and CD2AP) on Northern blots. The proximal/distal tubular marker genes (mFuc-TIX and uromodulin) were also reduced. In contrast, expression of NEPH1 and c-Myc was significantly elevated in the *mafB*$^{-/-}$ kidney. Pod1, a putative upstream regulator of *mafB*, was unchanged. The podocalyxin gene was unaffected (see Discussion). (B) Nephrin and podocin immunoreactivities were significantly reduced in the glomeruli of *mafB* homozygous mutant kidneys in comparison to their heterozygous littermates. The scale bars represent 20 μm. (C) Quantification of the RNA blotting analysis in panel A. The band intensities were quantified with ImageQuant version 5.2 (Molecular Dynamics) software and then normalized to GAPDH mRNA abundance. Three independent animals of each genotype were analyzed. Data are presented as the means ± SD. The statistical significances of the differences are indicated by asterisks (*, $P < 0.05$; **, $P < 0.01$ [Student's *t* test]).

unique feature of podocytes. Three major components (nephrin, podocin, and CD2 adaptor protein [CD2AP]) are required for slit diaphragm differentiation and function. Nephrin, the gene mutated in congenital nephritic syndrome of the Finnish type (NPHS1), encodes an immunoglobulin superfamily transmembrane protein that localizes to the slit diaphragm and joins the interdigitated pedicles (24). Podocin was identified as the gene mutated in autosomal recessive steroid-resistant nephritic syndrome (NPHS2) and is a membrane-integral protein belonging to the stomatin family (5). CD2AP is an Src homology 3 domain-containing protein that interacts directly with nephrin and is required for the assembly of the slit diaphragm (26, 27).

Given the kidney pathophysiology detected in the *mafB* null mutant mice, we asked whether MafB might lie in a common regulatory pathway leading to the expression of any of these kidney disease-related genes. We did so by comparing their expression in the neonatal kidneys of *mafB* heterozygous and homozygous mutant mice by RNA blot analysis. The results of these experiments demonstrated a significant reduction of nephrin, podocin, and CD2AP mRNAs in the homozygous mutant kidneys (Fig. 3A and C). In the glomeruli of *mafB* homozygous mutant kidneys, both nephrin and podocin immunoreactivities were significantly reduced in comparison to that of sibling heterozygotes (Fig. 3B). Since each of these genes is required for the normal development and function of the glomerulus, these data are fully congruent with the histological observations showing that podocytes in the homozygous mutant kidneys appear to be incompletely differentiated. We also observed an unexpected increase in NEPH1 expression in the homozygous neonatal mutant kidneys. NEPH1 is structurally related to nephrin and is known to interact with the C-terminal domain of podocin and nephrin (Fig. 3A and C and see Discussion) (3, 11, 43).

Given the perinatal anuria of *mafB* mutant newborns, we assayed the same kidneys for expression of podocalyxin, a podocyte membrane protein essential for foot process formation and maintaining the permeability of the glomerular filter (41). Podocalyxin mutant mice display a similar perinatal anuric phenotype due to lowered glomerular permeability (12). However, despite the similar anuric phenotype in the two mutants, podocalyxin expression was essentially unaffected by the homozygous *mafB* mutation (Fig. 3A and see Discussion). Taken together, these data show that MafB differentially regulates, directly or indirectly, the transcription of podocin, nephrin, and CD2AP in podocytes and that this regulation is essential for normal podocyte differentiation.

Renal tubular dysgenesis is accompanied by tubular epithelial cell death. We observed both proximal and distal tubular dysgenesis as well as renal cysts in *mafB* homozygous mutant kidneys (Fig. 2C to F), consistent with diminished expression of mFuc-TIX (CD15 synthase) and uromodulin (uromucoid, Tamm-Horsfall glycoprotein), which are proximal and distal tubule-specific markers, respectively (Fig. 3A and C) (25, 35, 48). To test the hypothesis that this tubular dysgenesis was caused by apoptotic tubular epithelial cell death, we carried out TUNEL assays to detect fragmented nuclear DNA in the kidneys of heterozygous and homozygous mutant neonatal mice.

The number of TUNEL-positive nuclei was significantly higher in *mafB* homozygous mutant kidneys than in those of their heterozygous littermates. The number of apoptotic cells increased predominantly in the tubule epithelium rather than in the glomerular region (Fig. 4A, B, and C). This observation indicates that a massive wave of cell death occurred in the renal tubuli of newborn homozygous mutant animals. As indicated above, MafB expression is detected specifically in podocytes but never in renal tubules (Fig. 1E to G), indicating that the increased apoptotic cell death of the tubular epithelial cells is not due to a cell-autonomous effect of MafB deficiency. We also observed significantly increased expression of c-Myc, a well-known apoptosis inducer, in the $mafB^{-/-}$ kidney (Fig. 3A) (9, 47), suggesting that tubular cell death may be induced through a c-Myc-dependent signaling pathway.

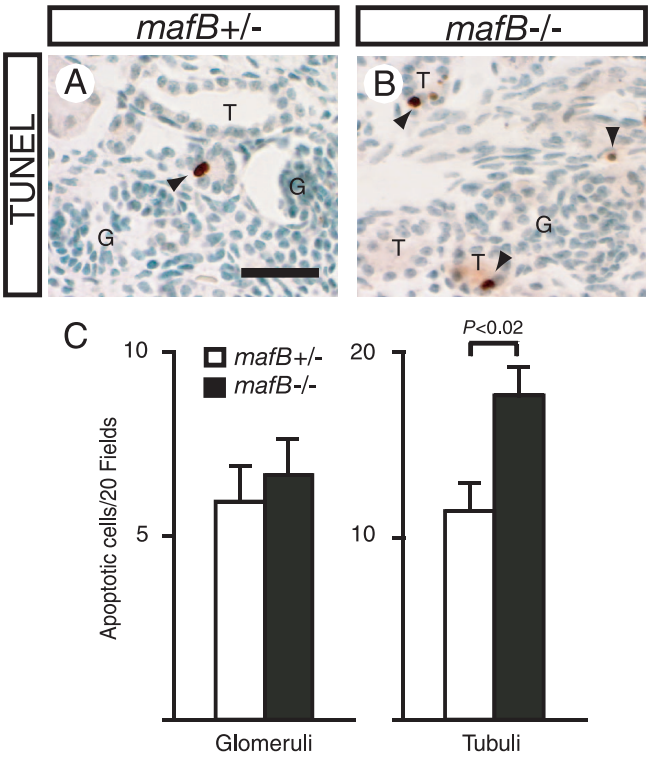

FIG. 4. Increased apoptosis in the kidneys of $mafB^{-/-}$ mice. (A and B) TUNEL-positive cells in $mafB^{+/-}$ and $mafB^{-/-}$ kidneys (indicated by arrowheads), respectively, were predominantly observed in the tubular cells of $mafB^{-/-}$ kidneys, whereas significantly fewer tubule cells are TUNEL positive in $mafB^{+/-}$ kidneys (T, tubule; G, glomerulus). The scale bar is 20 μm. (C) TUNEL-positive cells were counted in 20 randomly selected fields within the periglomerular area or cortical interstitium and were then recorded as TUNEL-reactive cells/20 fields. For each genotype, one central section from each of four kidneys from two different pups was analyzed. The data were recorded as means ± SD. The statistical significance of differences was determined by Student's *t* test.

MafB is expressed in a subpopulation of mature macrophages and is required for expression of F4/80. It was previously reported that MafB is expressed specifically in myelomonocyte lineage hematopoietic cells and was both necessary and sufficient to induce monocytic differentiation of transformed avian myeloblast cells in culture (23, 44). To examine hematopoietic lineage-specific MafB expression in vivo, we first monitored GFP expression in fetal liver cells recovered

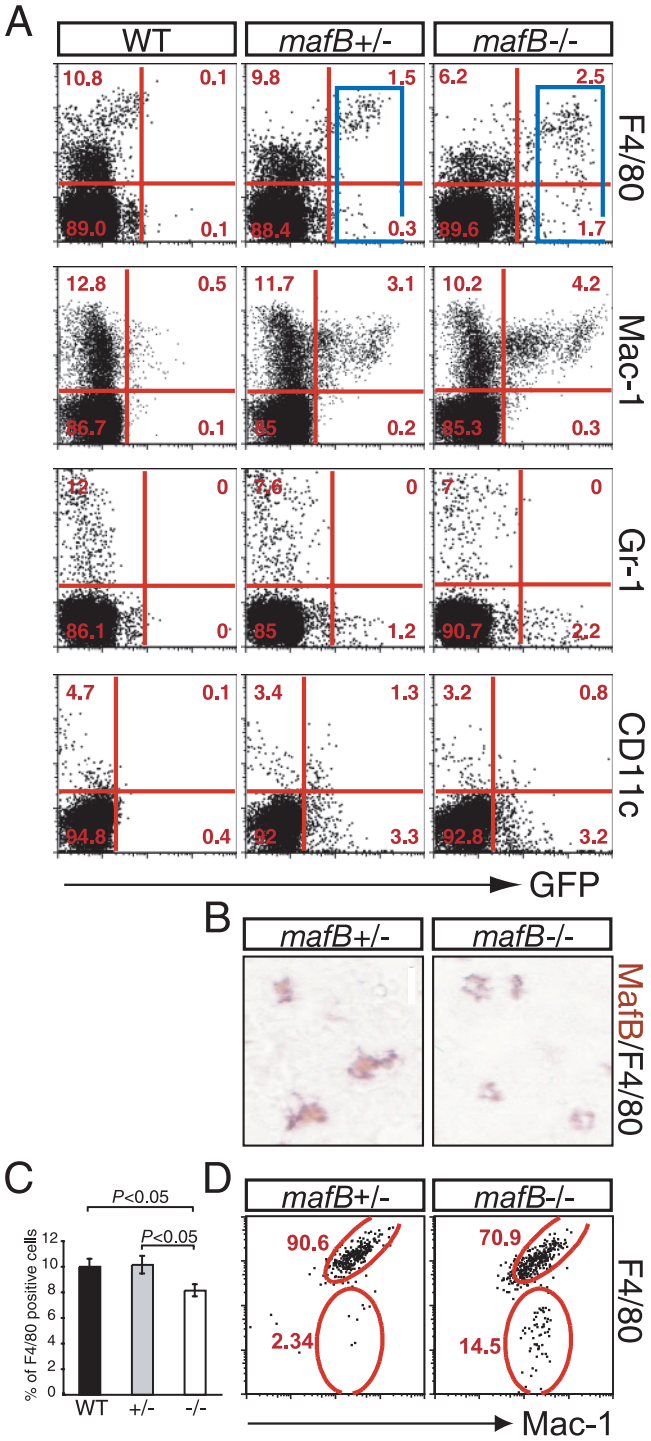

FIG. 5. Flow cytometric analysis of e14.5 fetal liver hematopoietic cells. (A) Single-cell suspensions were prepared from the livers of wild-type (WT) mice (+/+) or heterozygous (*mafB*$^{+/-}$) or homozygous (*mafB*$^{-/-}$) mutant e14.5 embryos. The cells were stained with PE- or APC-conjugated primary antibodies (indicated on the right) and then analyzed by flow cytometry. The profiles display GFP fluorescence on the horizontal axis and antibody-mediated PE or APC fluorescence on the vertical axis. The percentage of cells in each of the four quadrants is indicated. Specificities of the antibodies are as follows: F4/80, differentiated macrophage; Mac-1, monocyte-macrophage lineage; Gr-1, granulocytes; CD11c, dendritic cells. (B) MafB and F4/80 double immunostaining on frozen sections of e14.5 fetal liver from each genotype. In the *mafB*$^{+/-}$ control, MafB and F4/80 expression is nicely colocalized, whereas MafB immunoreactivity was absent in *mafB*$^{-/-}$ fetal livers. (C) In e14.5 fetal liver cells from *mafB*$^{-/-}$ mice, the total population of F4/80-positive cells was slightly reduced in comparison to the number recovered in either *mafB*$^{+/-}$ or wild-type mice. (D) F4/80 and Mac-1 expression profile in GFP-positive (MafB-expressing) macrophages. A total of 1.1% of GFP-positive cells (blue gates in panel A) from each genotype were analyzed. In the *mafB*$^{-/-}$ cells, an increase of F4/80$^-$ Mac-1$^+$ premature macrophages and a reduction of F4/80$^+$ Mac-1$^+$ mature macrophages were observed.

from *mafB* heterozygous embryos at embryonic day 14.5 (e14.5) by flow cytometry in parallel with several hematopoietic lineage-specific markers. Interestingly, most of the GFP-positive cells in the *mafB*$^{+/-}$ e14.5 fetal liver were stained with both terminally differentiated macrophage-specific antigen F4/80 and myelomonocyte-specific antigen Mac-1 (Fig. 5, middle column), whereas GFP-positive cells in the heterozygotes were largely negative for granulocyte-specific antigen Gr-1, the myeloid-related dendritic cell marker CD11c, Ter119-positive erythroid cells, and CD4-, CD8-, and CD19-positive lymphoid lineages (Fig. 5A and data not shown). GFP-positive cells were observed in both negative and positive fractions for antigen-presenting cell marker MHC class II (data not shown). Immunohistochemical analysis of MafB plus F4/80 showed that endogenous MafB expression colocalized with the macrophage-specific antigen F4/80 in the e14.5 heterozygous fetal liver (Fig. 5B). Thus, these observations suggest that MafB is most specifically expressed in F4/80- and Mac-1-positive macrophages in vivo.

We next asked if hematopoietic deficiencies are observed in *mafB* null mutant hematopoietic cells. When homozygous mutant e14.5 fetal livers were examined simultaneously for MafB and F4/80, although MafB immunoreactivity was absent, as expected, F4/80 staining persisted (Fig. 5B). Interestingly, however, in flow cytometric analysis of e14.5 homozygous mutant fetal liver cells, the absolute number of F4/80-expressing cells (8% ± 0.45% [n = 8]) was slightly but reproducibly reduced in comparison to that of the wild type (10% ± 0.42% [n = 9]) (Fig. 5A and C). Furthermore, in the mutants, we observed a significant increase in the number of F4/80^{lo} GFP^{hi} and F4/80$^-$ GFP^{hi} cells in a continuum with F4/80^{hi} GFP^{hi} cells (Fig. 5A, blue gate). Those MafB-deficient cells are Mac-1$^+$/CD11c$^-$ macrophages (Fig. 5A, Mac-1 and CD11c plot), and thus, these data suggest that the MafB deficiency causes the suppression of F4/80 expression in Mac-1$^+$ macrophages (Fig. 5A). To attempt to determine the fate of MafB-deficient macrophages, we analyzed the F4/80 and Mac-1 expression profiles among the GFP-bright (highly MafB-expressing) macrophages in both *mafB*$^{+/-}$ and *mafB*$^{-/-}$ e14.5 fetal liver cells (Fig. 5A, blue gates). In the homozygous mutant, F4/80$^-$ Mac-1$^+$ immature macrophages are significantly more abundant (up to 14.5% of the GFP$^+$ fraction), whereas comparable heterozygous fetal livers had only 2.3% of fetal liver cells in the same fraction, confirming the hypothesis that MafB deficiency suppresses F4/80 expression in MafB-expressing macrophages (Fig. 5D). At the same time, the Mac-1$^+$ total macrophage population as well as all other lineage markers tested (Gr-1, CD11c, CD4, CD8, CD19, Ter-119, and MHC class II) displayed no differ-

ences (Fig. 5A and data not shown), suggesting that MafB influences F4/80 expression in MafB-expressing macrophages in a cell-autonomous manner.

The reduction in the F4/80$^+$ population and concurrent increase of F4/80$^-$ GFP$^+$ cells in the *mafB* homozygotes was even more prominent in newborn peripheral blood and spleens (Fig. 6A and C), while the total Mac-1$^+$ macrophage population was hardly affected (Fig. 6C). As expected, the accumulation of F4/80$^-$ Mac-1$^+$ antigen in the GFP$^+$ (MafB-expressing) macrophages significantly increased in the homozygous mutant spleen cells (Fig. 6B) and peripheral blood (data not shown).

We next assessed whether e14.5 fetal liver cells in the *mafB* mutants were altered in the normal spectrum of erythroid and myeloid CFU by in vitro colony assays. Only few differences were observed in CFU-erythrocyte, CFU-granulocyte/macrophage, and CFU-granulocyte/erythrocyte/macrophage/megakaryocyte in erythropoietin-, stem cell factor-, interleukin-3 (IL-3)-, and granulocyte colony-stimulating factor-supplemented media (data not shown). These data suggest that while MafB is important for the presentation of the F4/80 terminal differentiation marker and its expression in MafB-expressing mature macrophages, MafB is not necessary for the development of macrophages.

MafB is indispensable for F4/80 expression in nonadherent macrophages. We next examined the differentiation potential of fetal liver macrophages in primary cultures. The traditional view of the mononuclear phagocyte system suggests that circulating monocytes enter peripheral tissues to become macrophages, implying that their direct attachment to extracellular substrates could be a critical cue for macrophage differentiation. It is well established that cell-adhesive interactions with the extracellular matrix transmit differentiation signals through integrin-mediated pathways in monocytes (7). In contrast, cell adherence to plastic tissue culture dishes results in a rapid induction of multiple mature macrophage-specific genes, suggesting that in an adhesive plastic petri dish, macrophage progenitor cells might be induced to undergo differentiation (29). Since blood cells in hematopoietic tissues are exposed to constant blood flow-mediated shear stress, this dynamic process could normally prevent tight interactions between myelomonocytic cells and the extracellular matrix (10). We therefore attempted to exclude such external differentiation signals arising from cell adhesion and to reconstitute a physiological hematopoietic environment by culturing e14.5 fetal liver cells on nonadhesive dishes coated with hydrophilic polymers (Hydrocell; Cell Seed, Tokyo, Japan). Cell adhesion is completely inhibited on the hydrophilic surface of these dishes. We then compared the differentiation profiles of these cells to those of normal (adhesive dish-cultured) macrophages.

Interestingly, in the *mafB* mutant fetal liver cells grown under nonadhesive conditions (Fig. 7A, right panel, blue line), most failed to express F4/80, although 90% of the wild-type cells under identical conditions produced F4/80$^+$ mature macrophages (Fig. 7A, left panel, blue line). Conversely, under adherent conditions, more than 85% of the macrophages derived from either the wild-type or *mafB* mutants differentiated into F4/80-expressing cells (Fig. 7A, red lines in the left and right panels). Real-time PCR analysis of nonadherent macrophages showed a 50% reduction in F4/80 mRNA levels in the homozygous mutant macrophages (Fig. 7C). Following the time course on nonadherent dishes, the MafB deficiency suppressed F4/80 expression from day 2 onward, although Mac-1 expression was unaffected (Fig. 7B).

To further confirm F4/80 suppression in the *mafB* homozygous mutant macrophages under other nonadherent conditions, we analyzed e14.5 fetal liver-derived macrophages in methylcellulose supplemented with M-CSF. A total of 81.1% of *mafB* homozygous mutant fetal liver cells gave rise to GFP$^+$ macrophages, although most of them failed to express F4/80 (Fig. 8A to D), while under identical conditions, 92% of wild-type cells gave rise to F4/80$^+$ macrophages (Fig. 8C). These combined results demonstrate that MafB is required for F4/80 expression under nonadherent conditions.

To test the hypothesis that MafB directly regulates the F4/80 gene, we performed reporter assays using a 668-bp F4/80 promoter/luciferase construct that was cotransfected with a MafB expression vector (36, 37). A well-conserved MARE half-site (CTTTCTGCTGAGTTGCCA [underlined letters are the consensus MARE half-site]) from −130 to −113 bp (37) was identified within the F4/80 promoter. The F4/80-directed reporter was activated (ca. 10-fold) by MafB cotransfection in a dose-dependent manner after transfection into the murine macrophage cell line RAW264.7, suggesting that MafB directly regulates the F4/80 promoter region (Fig. 8E).

For characterization of their differentiated phenotype, fetal liver-derived macrophages (cultured on nonadherent dishes) were assessed for their ability to engulf Nile red fluorescent carboxylate-modified microspheres; the mean overall phagocytic activities of macrophages derived from the wild type and heterozygous and homozygous *mafB* mutants were indistinguishable (data not shown). The production of nitric oxide and inflammatory/anti-inflammatory cytokines such as IL-6, IL-12, and IL-10 treated with lipopolysaccharide was also quantified. No significant difference in production of those cytokines was observed (data not shown), and differences in nitric oxide production were minimal (our unpublished observations), suggesting that germ line inactivation of *mafB* does not significantly affect conventional macrophage functions.

DISCUSSION

In this study, we report that the kidneys of mice in which both *mafB* alleles have been disrupted display renal dysgenesis and non-cell-autonomous apoptotic cell death in tubular epithelial cells. The substantial reduction of tubular epithelial cell populations in the renal medulla and the accompanying increase of renal mesenchymal cells caused a visible dystrophic appearance of the *mafB*$^{-/-}$ kidney. In addition, the expression of kidney disease-related genes nephrin, podocin, and CD2AP were significantly reduced in *mafB*$^{-/-}$ mice. Recently, *Kr*^{ENU} mutant mice were reported to display abnormal foot process formation, although differences in the expression levels of these same kidney disease-related genes were minimal (39). These observations are consistent with the hypothesis that the *kr*^{ENU} mutation is a hypomorphic allele of the *mafB* gene. The *kr*^{ENU} mutation, a missense mutation at a conserved asparagine residue in the MafB DNA binding domain, is therefore likely to retain partial function in the absence of DNA binding, possibly through interactions with other bZip transcription factors or cofactors. One recent report indeed

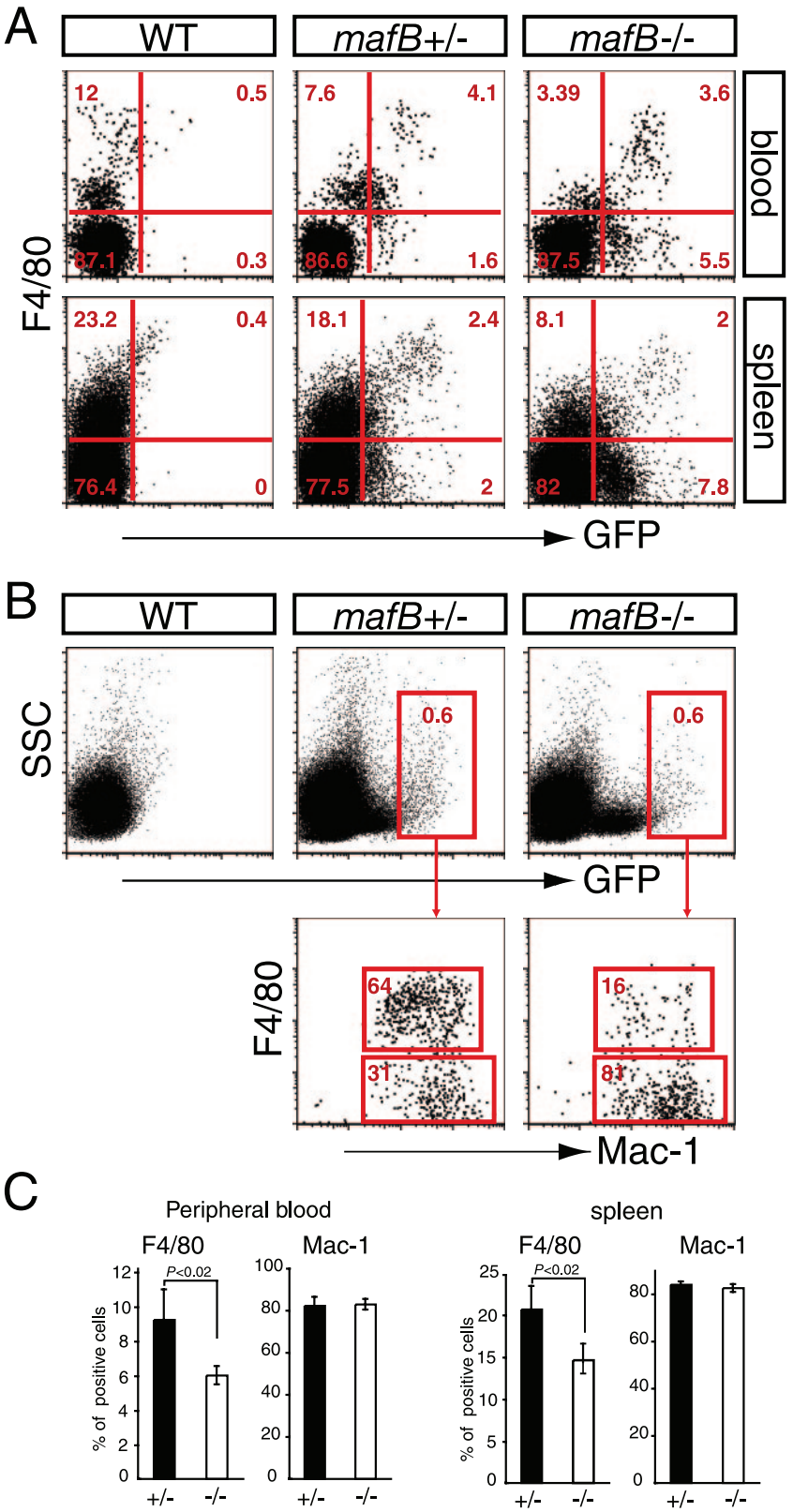

FIG. 6. F4/80 expression is suppressed in MafB-deficient macrophages. (A and C) Reduction of the F4/80-positive population and the increase in the GFP$^+$ F4/80$^-$ population in neonatal peripheral blood and spleen cells. The Mac-1-positive macrophage population was unaffected (C). (B) F4/80 and Mac-1 expression profiles in GFP-positive (MafB-expressing) macrophages. A total of 0.6% of GFP-positive cells (red gates in B) from each genotype were analyzed. In the *mafB*$^{-/-}$ cells, an increase of F4/80$^-$ Mac-1$^+$ premature macrophages and a reduction of F4/80$^+$ Mac-1$^+$ mature macrophages were observed. Seven independent animals of each genotype were analyzed. The data were recorded as means ± SD. The statistical significance of differences was determined by Student's *t* test. WT, wild type.

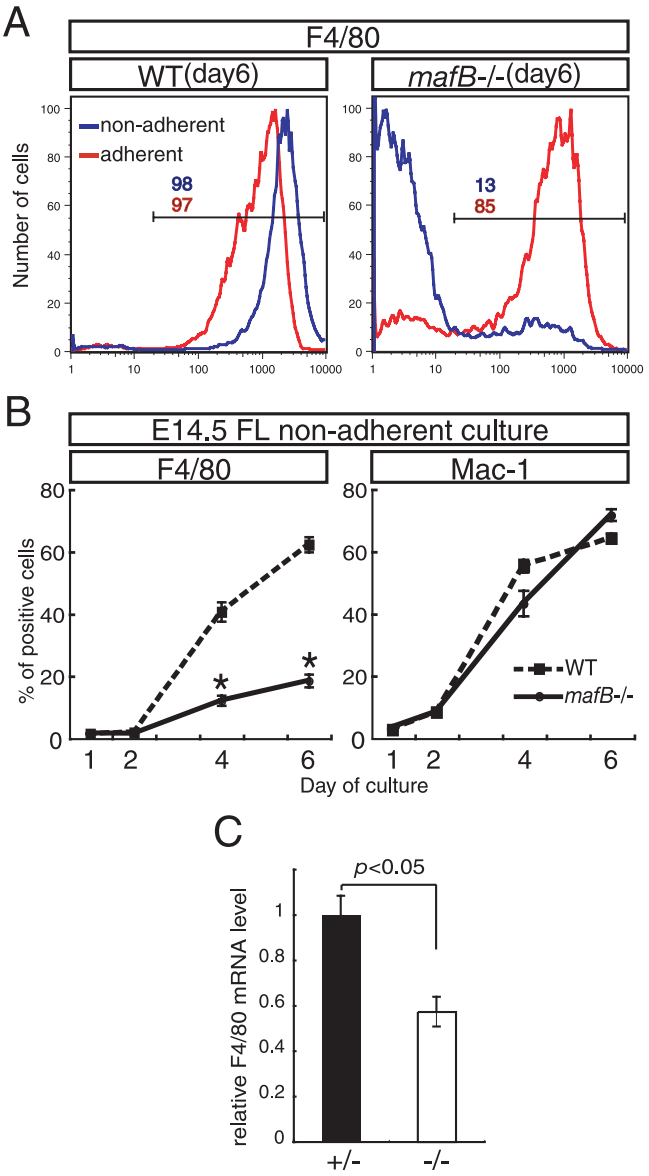

FIG. 7. Failure to induce F4/80 in nonadherent *mafB*$^{-/-}$ macrophages. (A) The *mafB* mutant fetal liver-derived macrophages (right panel, blue line) failed to express F4/80 immunoreactivity when cultured under nonadherent conditions in the presence of M-CSF for 6 days, although 98% of wild-type (WT) fetal liver cells generated F4/80-positive mature macrophages (left panel, blue line). When wild-type or *mafB*$^{-/-}$ cells were cultured on adherent substrates (red lines), more than 85% of the hematopoietic cells of both genotypes differentiated into F4/80-positive cells. (B) When cultured under nonadherent conditions, MafB deficiency suppressed F4/80 expression from day 2 onward, although Mac-1 expression was not affected. FL, fetal liver. (C) Real-time PCR analysis of nonadherent macrophages showed a 50% reduction of F4/80 mRNA expression in the homozygous mutant macrophages. Seven independent animals of each genotype were analyzed. The data were recorded as means ± SD. The statistical significance of differences was determined by Student's *t* test.

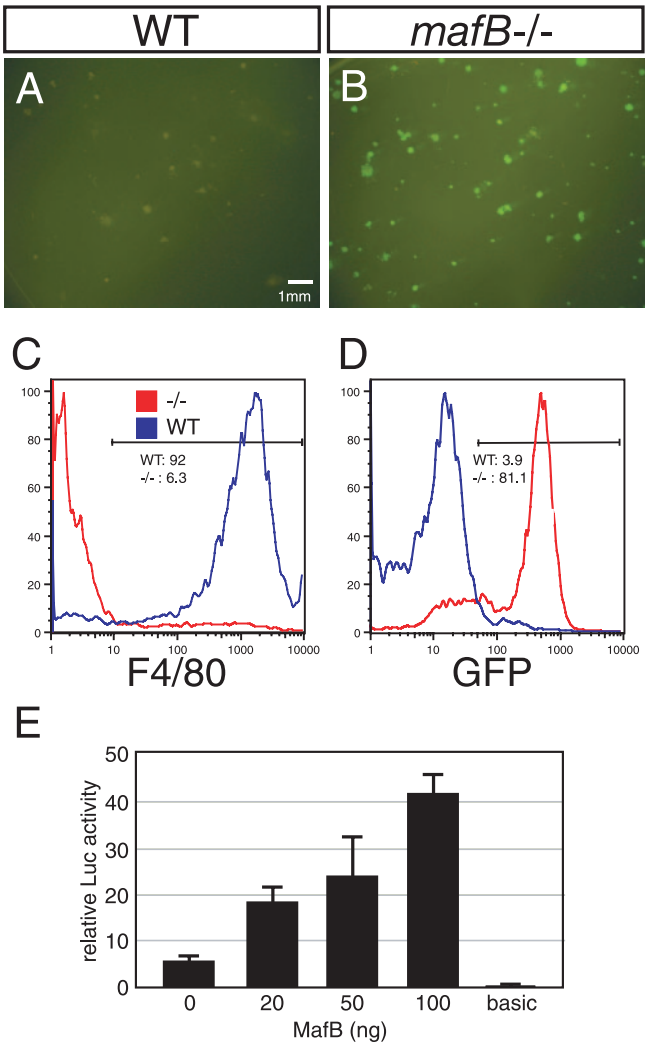

FIG. 8. *mafB*$^{-/-}$ macrophages derived from methylcellulose culture fail to induce F4/80 expression. In methylcellulose medium supplemented with M-CSF, 81.1% of *mafB*$^{-/-}$ e14.5 fetal liver cells gave rise to GFP-positive macrophages (A, B, and D). A total of 92% of e14.5 wild-type (WT) fetal liver cells gave rise to F4/80-positive macrophages, whereas most *mafB*$^{-/-}$ fetal liver cells failed to induce F4/80 expression (C). (E) Cotransfection reporter assay using the 668-bp F4/80 promoter reporter and the MafB expression vector. Luciferase (Luc) activity was significantly activated by cotransfection of the MafB expression vector in a dose-dependent manner in the murine macrophage cell line RAW264.7.

showed that *kr*^{ENU} was able to form dimers with wild-type MafB and *trans*-activate a reporter gene (40). The *mafB*$^{-/-}$ mice reported here, representing a complete loss of MafB function, poorly activate the nephrin, podocin, and CD2AP genes, demonstrating that they are clearly under the (direct or indirect) influence of MafB in developing podocytes of the kidney.

We also observed increased NEPH1 expression in *mafB*$^{-/-}$ neonatal kidneys. NEPH1 is a molecule related to nephrin and belongs to a family of three closely related proteins that interact with the C-terminal domain of podocin (11, 43). NEPH1 forms a heterooligomeric complex with nephrin in the plane of the membrane that appears to interact across the foot process intercellular junction (3). These data suggest that the inhibition of podocin and nephrin might induce compensatory NEPH1 expression for the maintenance of the slit diaphragm structure in *mafB*$^{-/-}$ neonatal kidneys.

Deficiencies in nephrin, podocin, or CD2AP commonly lead

to nephrosis and massive proteinuria, so the observed perinatal anuria might not simply represent a reduction in the expression of these genes. Podocalyxin is a podocyte membrane protein with a highly charged cytoplasmic tail. On mature podocytes, podocalyxin is essential for foot process formation and for maintaining the spacing between the interdigitating foot processes by charge repulsion (41). In podocalyxin mutant mice, the reduced permeability of the glomerular filter due to increased tight junctions between adjacent podocytes leads to the observed perinatal anuria phenotype (12). Despite a similar anuric phenotype detected in *mafB* mutant newborns, podocalyxin expression was barely affected in the *mafB* mutant kidney (Fig. 3A), suggesting that the phenotypes observed in the *mafB* and podocalyxin mutants lie in different biochemical and genetic pathways. It is nonetheless possible that MafB regulates other (undefined) genes that are required to preserve glomerular permeability.

To our surprise, we also observed severe proximal and distal tubular dysgenesis, which are equally likely to be the direct cause of the observed anuric phenotype in the *mafB*$^{-/-}$ animals. MafB is not expressed in renal tubuli as reflected by GFP immunohistochemistry, in accord with previously reported in situ hybridization studies (18, 39). Despite this lack of *mafB* expression, TUNEL staining clearly demonstrated significantly increased apoptotic cell death of renal tubular epithelial cells in *mafB*$^{-/-}$ kidneys, leading to the conclusion that tubular apoptosis is a non-cell-autonomous effect of the MafB deficiency.

In early morphogenesis of the kidney and urinary tract, the elongation and branching of the nephric duct are promoted by a number of humoral factors secreted from the metanephric mesenchyme, including primitive glomerular epithelial cells (6, 32). Although MafB expression is first detected at a relatively late stage of kidney development, it is intriguing to hypothesize that the mature podocyte may secrete a humoral factor that is required for the maintenance of tubular epithelial cell growth and differentiation. It may thus be particularly germane that we also observed significantly increased expression of c-Myc, a well known apoptosis inducer, in *mafB*$^{-/-}$ kidneys (Fig. 3A). Autosomal dominant polycystic kidney disease, one of the most frequent human genetic disorders that constitutes a major cause of end-stage renal failure worldwide, is associated with increased levels of c-Myc (9). Indeed, a model for the human disease, the autosomal dominant polycystic kidney disease transgenic mouse, was generated by targeted overexpression of c-Myc to the renal tubular epithelium, and this mouse displays severe renal anomalies characteristic of polycystic kidney disease (47). Thus, we suggest that the tubular dysgenesis and cyst formation observed in the *mafB*$^{-/-}$ kidney may be mediated by c-Myc-induced apoptosis. Since their GFP fluorescence will enable us to collect podocytes from *mafB*$^{-/+}$ or *mafB*$^{-/-}$ kidneys by flow cytometry, we may be able to identify candidate target genes of MafB, including this hypothetical tubular growth factor.

Although it has been shown that MafB is expressed selectively in myelomonocytic cells and plays key roles in differentiating macrophages, a similar demonstration has never been confirmed in vivo. In this report, we show that MafB was expressed in a subpopulation of differentiated macrophages. Flow cytometric analysis of fetal liver cells revealed that MafB was expressed in distinct subsets of differentiated macrophages that expressed Mac-1 and F4/80. In *mafB*$^{-/-}$ mice, a substantial proportion of fetal liver, neonatal spleen, and peripheral macrophages failed to express F4/80, indicating that MafB is required for the full differentiation of this distinct subset of macrophages.

F4/80, a member of the epidermal growth factor-TM7 (seven-transmembrane-domain) family, has been established as a specific cell surface marker for murine macrophages (2, 31). The precursor of tissue macrophages, the blood monocyte, is known to express less F4/80 than its mature counterparts (14). Although the function of F4/80 in macrophages remains unknown, one recent report demonstrated that F4/80 expression in APCs was essential for the induction of immunological tolerance by generating antigen-specific efferent regulatory T (T reg) cells that suppress antigen-specific immunity (28). During peripheral immunotolerance induction, F4/80^{+} APCs first appear in the bloodstream and then circulate to the splenic marginal zone, where they interact with NK-T cells, which in turn generate T reg cells. Moreover, F4/80 expression in blood APCs is essential for T reg induction, presumably through the F4/80-mediated direct interaction between the two different cell types (28). In the present study, we showed that MafB is essential for F4/80 expression, especially in nonadherent macrophages. Given the importance of F4/80 expression in circulating APCs for the induction of peripheral immunotolerance, it is intriguing to hypothesize an essential role for MafB as a regulator of immunological tolerance by maintaining F4/80 expression in circulating tolerogenic APCs.

Assuming a direct regulatory interaction between MafB and F4/80, we examined the sequence of the mouse F4/80 proximal promoter region. One site identified is a well-conserved half-site MARE (actual sequence, CTTTCTGCTGAGTTGCCA, where the underlined letters are the consensus MARE half-site) from −130 to −113 bp of the F4/80 promoter. A recent report showed that 5′ AT-rich MARE half-sites retain Maf binding site potency as strong as the classical palindromic MARE (49). Moreover, it was reported recently that a serial deletion study of that promoter revealed strong enhancer activity between −187 and −117 bp, which includes the predicted MARE element (37). It is therefore quite plausible that MafB binds to the F4/80 promoter at that site to stimulate F4/80 transcription in mature macrophages.

In summary, the results presented here demonstrate an essential role for MafB in the development of the mature glomerulus, in renal tubules (unexpectedly), and in F4/80-expressing macrophages. Further analysis to determine the biological consequences of diminished F4/80 expression in the MafB-deficient macrophages, especially in adolescent animals, is ongoing.

ACKNOWLEDGMENTS

We thank T. Kuroha and A. Godo for excellent assistance and discussion.

This work was supported in part by grants-in-aid from the Ministry of Education, Science, Sports, and Culture; the Japanese Society for Promotion of Science (RFTF); NIH grants GM28896 and CA80088 (J.D.E. and T.M.); and the Genome Network Project from the Ministry of Education, Culture, Sports, Science, and Technology, Japan (S.T.).

REFERENCES

1. **Abrahamson, D.** 1991. Glomerulogenesis in the developing kidney. Semin. Nephrol. **11:**375–389.

2. **Austyn, J. M., and S. Gordon.** 1981. F4/80, a monoclonal antibody directed specifically against the mouse macrophage. Eur. J. Immunol. **11:**805–815.
3. **Barletta, G., I. A. Kovari, R. K. Verma, D. Kerjaschkil, and L. B. Holzman.** 2003. Nephrin and Neph1 co-localize at the podocyte foot process intercellular junction and form cis hetero-oligomers. J. Biol. Chem. **278:**19266–19271.
4. **Blanchi. B., L. M. Kelly, J. C. Viemari, I. Lafon, H. Burnet, M. Bevengut, S. Tillmanns, L. Daniel, T. Graf, G. Hilaire, and M. H. Sieweke.** 2003. MafB deficiency causes defective respiratory rhythmogenesis and fatal central apnea at birth. Nat. Neurosci. **10:**1091–1100.
5. **Boute, N., O. Gribouval, S. Roselli, F. Benessy, H. Lee, A. Fuchshuber, K. Dahan, M. C. Gubler, P. Niaudet, and C. Antignac.** 2000. NPHS2, encoding the glomerular protein podocin, is mutated in autosomal recessive steroid-resistant nephrotic syndrome. Nat. Genet. **24:**349–354.
6. **Clark, A. T., and J. F. Bertram.** 1999. Molecular regulation of nephron endowment. Am. J. Physiol. Renal Physiol. **276:**F485–F497.
7. **Coccia, E. M., N. Del Russo, E. Stellacci, U. Testa, G. Marziali, and A. Battistini.** 1999. STAT1 activation during monocyte to macrophage maturation: role of adhesion molecules. Int. Immunol. **11:**1075–1083.
8. **Cordes, S. P., and G. S. Barsh.** 1994. The mouse segmentation gene *kr* encodes a novel basic domain-leucine zipper transcription factor. Cell **79:** 1025–1034.
9. **Couillard, M., R. Guillaume, N. Tanji, V. D'Agati, and M. Trudel.** 2002. c-myc-induced apoptosis in polycystic kidney disease is independent of FasL/Fas interaction. Cancer Res. **62:**2210–2214.
10. **Davies, P. F.** 1995. Flow-mediated endothelial mechanotransduction. Physiol. Rev. **75:**519–560.
11. **Donoviel, D. B., D. D. Freed, H. Vogel, D. G. Potter, E. Hawkins, J. P. Barrish, B. N. Mathur, C. A. Turner, R. Geske, C. A. Montgomery, M. Starbuck, M. Brandt, A. Gupta, R. Ramirez-Solis, B. P. Zambrowicz, and D. R. Powell.** 2001. Proteinuria and perinatal lethality in mice lacking NEPH1, a novel protein with homology to NEPHRIN. Mol. Cell. Biol. **21:**4829–4836.
12. **Doyonnas, R., D. B. Kershaw, C. Duhme, H. Merkens, S. Chelliah, T. Graf, and K. M. McNagny.** 2001. Anuria, omphalocele, and perinatal lethality in mice lacking the CD34-related protein podocalyxin. J. Exp. Med. **194:**13–27.
13. **Eichmann, A., A. Grapin-Botton, L. Kelly, T. Graf, N. M. Le Douarin, and M. Sieweke.** 1997. The expression pattern of the mafB/kr gene in birds and mice reveals that the kreisler phenotype does not represent a null mutant. Mech. Dev. **65:**111–122.
14. **Gordon, S., L. Lawson, S. Rabinowitz, P.R. Crocker, L. Morris, and V. H. Perry.** 1992. Antigen markers of macrophage differentiation in murine tissues. Curr. Top. Microbiol. Immunol. **181:**1–37.
15. **Hamada, M., T. Moriguchi, T. Yokomizo, N. Morito, C. Zhang, and S. Takahashi.** 2003. The mouse *mafB* 5′-upstream fragment directs gene expression in myelomonocytic cells, differentiated macrophage and the ventral spinal cord in transgenic mice. J. Biochem. **134:**203–210.
16. **Holzman, L. B., P. L. St. John, I. A. Kovari, R. Verma, H. Holthofer, and D. R. Abrahamson.** 1999. Nephrin localizes to the slit pore of the glomerular epithelial cell. Kidney Int. **56:**1481–1491.
17. **Hooper, M., K. Hardy, A. Handyside, S. Hunter, and M. Monk.** 1987. HPRT-deficient (Lesch-Nyhan) mouse embryos derived from germline colonization by cultured cells. Nature **326:**292–295.
18. **Imaki, J., H. Onodera, K. Tsuchiya, T. Imaki, T. Mochizuki, T. Mishima, K. Yamashita, K. Yoshida, and M. Sakai.** 2000. Developmental expression of *maf-1* messenger ribonucleic acids in rat kidney by *in situ* hybridization histochemistry. Biochem. Biophys. Res. Commun. **272:**777–782.
19. **Kajihara, M., S. Kawauchi, M. Kobayashi, H. Ogino, S. Takahashi, and K. Yasuda.** 2001. Isolation, characterization, and expression analysis of zebrafish large Mafs. J. Biochem. **129:**139–146.
20. **Kataoka, K., K. T. Fujiwara, M. Noda, and M. Nishizawa.** 1994. MafB, a new Maf family transcription activator that can associate with Maf and Fos but not with Jun. Mol. Cell. Biol. **14:**7581–7591.
21. **Kataoka. K., M. Noda, and M. Nishizawa.** 1994. Maf nuclear oncoprotein recognizes sequences related to an AP-1 site and forms heterodimers with both Fos and Jun. Mol. Cell. Biol. **14:**700–712.
22. **Kawauchi, S., S. Takahashi, O. Nakajima, H. Ogino, M. Morita, M. Nishizawa, K. Yasuda, and M. Yamamoto.** 1999. Regulation of lens fiber cell differentiation by transcription factor c-Maf. J. Biol. Chem. **274:**19254–19260.
23. **Kelly, L. M., U. Englmeier, I. Lafon, M. H. Sieweke, and T. Graf.** 2000. MafB is an inducer of monocytic differentiation. EMBO J. **19:**1987–1997.
24. **Kestila, M., U. Lenkkeri, M. Mannikko, J. Lamerdin, P. McCready, H. Putaala, V. Ruotsalainen, T. Morita, M. Nissinen, R. Herva, C. E. Kashtan, L. Peltonen, C. Holmberg, A. Olsen, and K. Tryggvason.** 1998. Positionally cloned gene for a novel glomerular protein—nephrin—is mutated in congenital nephritic syndrome. Mol. Cell **1:**575–582.
25. **Kudo, T., Y. Ikehara, A. Togayachi, M. Kaneko, T. Hiraga, K. Sasaki, and H. Narimatsu.** 1998. Expression cloning and characterization of a novel murine α1, 3-fucosyltransferase, mFuc-TIX, that synthesizes the Lewis x (CD15) epitope in brain and kidney. J. Biol. Chem. **273:**26729–26738.
26. **Lehtonen, S., A. Ora, V. M. Olkkonen, L. Geng, M. Zerial, S. Somlo, and E. Lehtonen.** 2000. In vivo interaction of the adaptor protein CD2-associated protein with the type 2 polycystic kidney disease protein, polycystin-2. J. Biol. Chem. **275:**32888–32893.
27. **Li, C., V. Ruotsalainen, K. Tryggvason, A. S. Shaw, and J. H. Miner.** 2000. CD2AP is expressed with nephrin in developing podocytes and is found widely in mature kidney and elsewhere. Am. J. Physiol. Renal Physiol. **279:**F785–F792.
28. **Lin, H. H., D. E. Faunce, M. Stacey, A. Terajewicz, T. Nakamura, J. Zhang-Hoover, M. Kerley, M. L. Mucenski, S. Gordon, and J. Stein-Streilein.** 2005. The macrophage F4/80 receptor is required for the induction of antigen-specific efferent regulatory T cells in peripheral tolerance. J. Exp. Med. **201:**1615–1625.
29. **Lin, T. H., A. Yurochko, L. Kornberg, J. Morris, J. J. Walker, S. Haskill, and R. L. Juliano.** 1994. The role of protein tyrosine phosphorylation in integrin-mediated gene induction in monocytes. J. Cell Biol. **126:**1585–1593.
30. **Minegishi, N., J. Ohta, H. Yamagiwa, N. Suzuki, S. Kawauchi, Y. Zhou, S. Takahashi, N. Hayashi, J. D. Engel, and M. Yamamoto.** 1999. The mouse GATA-2 gene is expressed in the para-aortic splanchnopleura and aorta-gonads and mesonephros region. Blood **93:**4196–4207.
31. **Morris, L., C. F. Graham, and S. Gordon.** 1991. Macrophages in haemopoietic and other tissues of the developing mouse detected by the monoclonal antibody F4/80. Development **112:**517–526.
32. **Moser, M., A. Pscherer, C. Roth, J. Becker, G. Mucher, K. Zerres, C. Dixkens, J. Weis, L. G. Woodford, R. Buettner, and R. Fassler.** 1997. Enhanced apoptotic cell death of renal epithelial cells in mice lacking transcription factor AP-2β. Genes Dev. **11:**1938–1948.
33. **Nishizawa, M., K. Kataoka, N. Goto, K. T. Fujiwara, and S. Kawai.** 1989. *v-maf*, a viral oncogene that encodes a "leucine zipper" motif. Proc. Natl. Acad. Sci. USA **86:**7711–7715.
34. **Niwa, H., K. Araki, S. Kimura, S. Taniguchi, S. Wakasugi, and K. Yamamura.** 1993. An efficient gene-trap method using poly A trap vectors and characterization of gene-trap events. J. Biochem. **113:**343–349.
35. **Oberg, K. C., J. P. Pestaner, L. Bielamowicz, and E. P. Hawkins.** 1999. Renal tubular dysgenesis in twin-twin transfusion syndrome. Pediatr. Dev. Pathol. **2:**25–32.
36. **Ogino, H., and K. Yasuda.** 1998. Induction of lens differentiation by activation of a bZIP transcription factor, L-maf. Science **280:**115–118.
37. **O'Reilly, D., M. Addley, C. Quinn, A. J. MacFarlane, S. Gordon, A. J. McKnight, and D. R. Greaves.** 2004. Functional analysis of the murine Emr1 promoter identifies a novel purine-rich regulatory motif required for high-level gene expression in macrophage. Genomics **84:**1030–1040.
38. **Ruben, R. J.** 1973. Development and cell kinetics of the *kreisler* (*kr-kr*) mouse. Laryngoscope **83:**1440–1468.
39. **Sadl, V. S., F. Jin, J. Yu, S. Cui, D. Holmyard, S. E. Quaggin, G. S. Barsh, and S. P. Cordes.** 2002. The mouse *Kreisler* (*Krml1*/*MafB*) segmentation gene is required for differentiation of glomerular visceral epithelial cells. Dev. Biol. **249:**16–29.
40. **Sadl, V. S., A. Sing, L. Mar, F. Jin, and S. P. Cordes.** 2003. Analysis of hindbrain patterning defects caused by the *kreisler*^{enu} mutation reveals multiple roles of *Kreisler* in hindbrain segmentation. Dev. Dynamics **227:**134–142.
41. **Schnabel, E., G. Dekan, A. Miettinen, and M. G. Farquhar.** 1989. Biogenesis of podocalyxin—the major glomerular sialoglycoprotein—in the newborn rat kidney. Eur. J. Cell Biol. **48:**313–326.
42. **Schwarz, K., M. Simons, J. Reiser, M. A. Saleem, C. Faul, W. Kriz, A. S. Shaw, L. B. Holzman, and P. Mundel.** 2001. Podocin, a raft-associated component of the glomerular slit diaphragm, interacts with CD2AP and nephrin. J. Clin. Investig. **108:**1621–1629.
43. **Sellin, L., T. B. Huber, P. Gerke, I. Quack, H. Pavenstadt, and G. Walz.** 2002. NEPH1 defines a novel family of podocin-interacting proteins. FASEB J. **17:**115–117.
44. **Sieweke, M. H., H. Tekotte, J. Frampton, and T. Graf.** 1996. MafB is an interaction partner and repressor of Ets-1 that inhibits erythroid differentiation. Cell **85:**49–60.
45. **Suzuki, N., N. Suwabe, O. Ohneda, N. Obara, S. Imagawa, X. Pan, H. Motohashi, and M. Yamamoto.** 2003. Identification and characterization of 2 types of erythroid progenitors that express GATA-1 at distinct levels. Blood **102:**3575–3583.
46. **Swaroop, A., J. Xu, H. Pawar, A. Jackson, C. Skolnick, and N. Agarwal.** 1992. A conserved retina-specific gene encodes a basic motif/leucine zipper domain. Proc. Natl. Acad. Sci. USA **89:**266–270.
47. **Trudel, M., V. D'Agati, and F. Constantini.** 1991. C-myc as an inducer of polycystic kidney disease in transgenic mice. Kidney Int. **39:**665–671.
48. **Wangsiripaisan, A., P. E. Gengaro, C. L. Edelstein, and R. W. Schrier.** 2001. Role of polymeric Tamm-Horsfall protein in cast formation: oligosaccharide and tubular fluid ions. Kidney Int. **59:**932–940.
49. **Yoshida, T., T. Ohkumo, S. Ishibashi, and K. Yasuda.** 2005. The 5′-AT-rich half site of Maf recognition element: a functional target for bZip transcription factor Maf. Nucleic Acids Res. **33:**3465–3478.
50. **Zhang, C., T. Moriguchi, M. Kajihara, R. Esaki, A. Harada, H. Shimohata, H. Oishi, M. Hamada, N. Morito, K. Hasegawa, T. Kudo, J. D. Engel, M. Yamamoto, and S. Takahashi.** 2005. MafA is a key regulator of glucose-stimulated insulin secretion. Mol. Cell. Biol. **25:**4969–4976.